THE JOURNAL OF NAVIGATION (2002), **55**, 305–322. © The Royal Institute of Navigation
DOI: 10.1017/S0373463302001741 Printed in the United Kingdom

Extending Coverage of DGPS by Considering Atmospheric Models and Corrections

Changdon Kee and Doohee Yun

(*Seoul National University*, *Korea*)

We have developed a local-area ionospheric time-delay model that consists of nominal and perturbation models. The nominal model describes the trends of ionospheric time delay over 1–2 days and uses nine parameters. The perturbation model describes rapid changes of ionospheric time delay over 2–3 hours and uses six parameters. All the parameters are estimated from raw data measured at one reference station, which has filters to estimate all the parameters of the local-area ionospheric time-delay model. With this model and Black's tropospheric time-delay model, we obtain compensated Differential GPS (DGPS) pseudo-range corrections by subtracting the atmospheric time-delay difference between the reference station and the user. We believed that the model could extend DGPS coverage. To check this, we analyzed experimental data. The results show that this algorithm not only improves DGPS positioning accuracy, but also extends DGPS coverage from 100 km to more than 400 km. We named this new algorithm the Seoul National University Differential GPS (SNUDGPS).

KEY WORDS

1. GPS. 2. DGPS. 3. Modelling.

1. INTRODUCTION. Differential GPS (DGPS) corrections are not accurate if the reference station is more than 100 km from the user (Klobuchar, 1995). This is because the error-generating environment of the reference station is different from that of a distant user, the so-called 'spatial de-correlation problem'. This problem derives from several error sources such as ephemeris error, multi-path, tropospheric time delay and ionospheric time delay. If we consider that Selective Availability (SA) remains set to zero and also that ionosphere activity is still close to the peak of the cycle, ionospheric time delay will be the largest error source. This time delay must therefore be corrected to extend DGPS coverage.

Our goal is to extend DGPS coverage by use of an atmospheric model with ionospheric and tropospheric parts. For the tropospheric part, we have used Black's model, because it is simple to compute. There are many ionospheric time-delay models such as Klobuchar's model (1987), Qiu and Lachapelle's model (1994), and the ionospheric time delay estimation in Wide Area Differential GPS (WADGPS) (Kee, 1995; Chao *et al.*, 1995). However, we could not find an appropriate model that would satisfy our requirement that the ionospheric time-delay model should be based on real-time measurements, and we wanted to use only one reference station to estimate the parameters. We therefore decided to develop our own ionospheric time-

https://doi.org/10.1017/S0373463302001741 Published online by Cambridge University Press

delay model with three design goals. The first is the size of the coverage area. The target size is the Korean peninsula, so we have named it the local-area ionospheric time-delay model. The second target is on-line parameter estimation; all parameters should be estimated from raw data that are measured at only one reference station. The last is a quick response to rapid changes of ionosphere activity. To achieve this, we built our local-area ionospheric time-delay model using two parts. One is a nominal model, which uses nine parameters and covers the tendency of ionospheric time delay over 1–2 days. The other is a perturbation model, which uses six parameters and describes rapid changes of ionospheric time delay over 2–3 hours that cannot be represented by the nominal model.

With this local-area ionospheric time-delay model and Black's model, we have modified the DGPS correction algorithm and named it the Seoul National University DGPS (SNUDGPS). Figure 1 shows an overview of SNUDGPS. Let us assume that

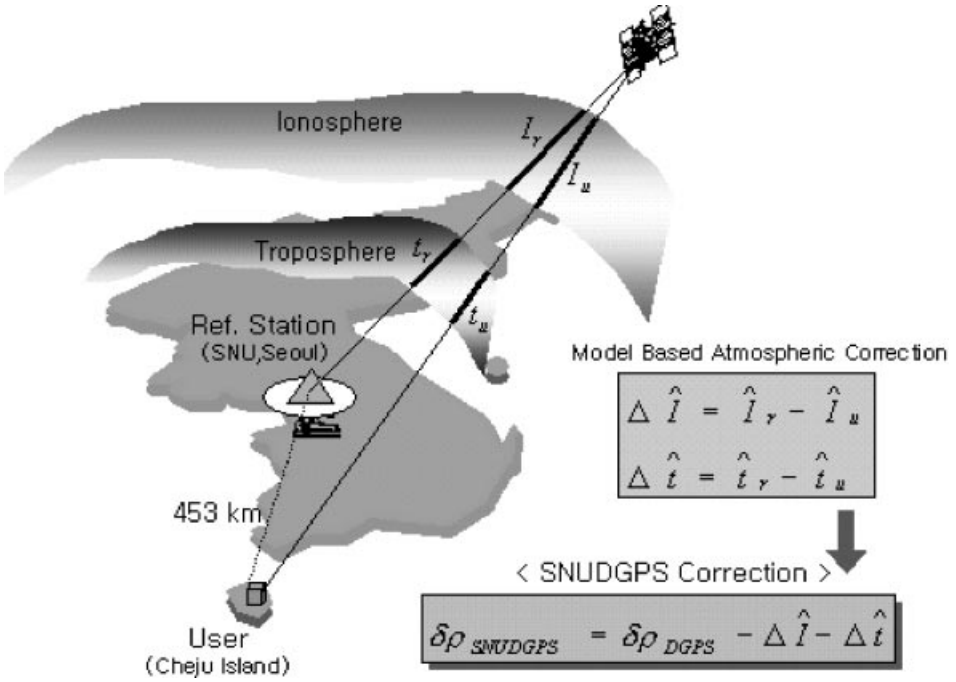


Figure 1. Overview of SNUDGPS.

the user is far away from a reference station. The user's ionospheric time delay (I_u) and tropospheric time delay (t_u) are different from those of the reference station (I_r, t_r). The DGPS pseudo-range correction ($\delta\rho_{DGPS}$) is therefore not accurate. However, if we use the local-area ionospheric time-delay model and the tropospheric time-delay model, we can calculate the differences ($\Delta\hat{I}$, $\Delta\hat{t}$) between the reference station and the user. We can then make a more accurate pseudo-range correction ($\delta\rho_{SNUDGPS}$) by subtracting these differences from the DGPS pseudo-range correction ($\delta\rho_{DGPS}$). If we use $\delta\rho_{SNUDGPS}$ instead of $\delta\rho_{DGPS}$ in the DGPS correction algorithm, it is anticipated that positioning performance can be improved and DGPS coverage can be extended to more than 100 km.

https://doi.org/10.1017/S0373463302001741 Published online by Cambridge University Press

To check whether SNUDGPS works well, we compared SNUDGPS with DGPS using the same experimental data. In the experiment, we placed a user 453 km away from the reference station to degrade DGPS positioning accuracy, and as expected, DGPS positioning errors were biased. However, there were no biases for SNUDGPS positioning errors. In addition, SNUDGPS positioning errors were smaller than DGPS errors. This is because atmospheric effects were removed successfully by the local-area ionospheric time-delay model and the tropospheric time-delay model.

This paper consists of theory, experimental results and conclusions. In the theory section, we introduce modelling coordinates and assumptions, the local-area ionospheric time-delay model, an on-line parameter estimation filter, and the principle of SNUDGPS. In the subsequent section, we present test results for the local-area ionospheric time-delay model, and we compare SNUDGPS with DGPS through experimental data analysis. Finally we draw conclusions.

2. THEORY.

2.1. *Modelling assumptions and coordinates.* We have used Klobuchar's assumptions in our ionospheric time-delay model (Klobuchar, 1987). Figure 2 shows these

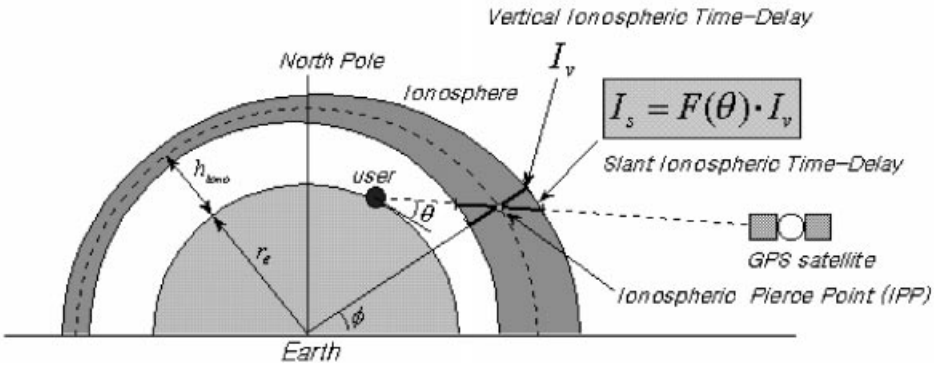


Figure 2. Ionospheric time-delay modelling assumptions.

assumptions; the ionosphere is assumed to be concentrated at the Ionospheric Pierce Point (IPP) and its average height (h_{iono}) is 350 km from the ground. Using ionospheric time-delay measurements at a number of IPPs from only one single reference station, we can develop a spatial ionospheric time-delay model, which covers a wider area than that of conventional DGPS and is appropriate for the size of Korean peninsular. This is the key concept of the paper. The real delay of the GPS signal is a slant ionospheric time delay, but this is not appropriate for the model because it varies according to satellite elevation angle; hence, the vertical ionospheric time delay should be used. Vertical and slant ionospheric time delays are related by an obliquity factor: $I_s = F \cdot I_v$, which is only a function of the satellite elevation angle: $F = F(\theta)$ (Qiu *et al.*, 1994).

As ionosphere activity is dominated by local time and geomagnetic latitude, the ionospheric time-delay model should be expressed in the coordinate of local time (t_{local}) and geomagnetic latitude (Φ_m) of the IPP. These can be calculated from GPS time, geographical latitude and longitude. We used the conversion algorithm of

https://doi.org/10.1017/S0373463302001741 Published online by Cambridge University Press

ARINC (1993). Figure 3 shows the modelling coordinates. In Figure 3, the local-area ionospheric time-delay model is expressed in terms of $\hat{I}_v$, which is a surface function of t_{local} and Φ_m. The parameter t_{local} is mapped from 0–24 hours to 0–2π in the local-area ionospheric time-delay model.

2.2. *Local-area ionospheric time-delay model.*

2.2.1. *Concept.* We built the local-area ionospheric time-delay model ($\hat{I}_v$) from two sub-models. Figure 4 shows that it is a sum of nominal and perturbation models; the nominal model ($\hat{I}_0$) describes ionosphere activity over 1–2 days, and the perturbation model ($\delta\hat{I}$) describes detailed ionosphere activity over 2–3 hours. In other words, the nominal model covers the low-frequency part, and the perturbation model covers the high-frequency part.

Our local-area ionospheric time-delay model can be expressed mathematically as Equation (1).

$$\hat{I}_v = \hat{I}_0 + \delta\hat{I}. \tag{1}$$

We used second-order spherical harmonics for $\hat{I}_0$ and second-order polynomials for $\delta\hat{I}$. The nominal model thus has nine parameters and the perturbation model has six parameters. The nominal model parameters are updated every five minutes and the perturbation model parameters are updated every minute. These update rates are sufficient because the ionospheric time delay changes slowly.

2.2.2. *Nominal ionospheric time-delay model and parameter estimation filter.* All the model parameters are estimated from measured slant ionospheric time delays. However, these contain L1/L2 inter-frequency biases (Wilson and Mannucci, 1994), which are generated because the electrical signal paths of the L1 and L2 circuits differ from each other. The biases exist both at the GPS satellite and the receiver (Wilson and Mannucci, 1993). They can be assumed to be nearly constant for about a month (Coco *et al.*, 1991). Thus, the measured slant ionospheric time delay (I_{s_m}) can be formulated as Equation (2).

$$I_{s_m} = I_s + I_{b_{RX}} - I_{b_{TX}} = I_{v_m} \cdot F(\theta) + I_{b_{RX}} - I_{b_{TX}}. \tag{2}$$

In Equation (2), the vertical ionospheric time delay measurements (I_{v_m}) do not contain any L1/L2 inter-frequency bias, and the nominal model ($\hat{I}_0$) parameters should be estimated from vertical ionospheric time delay measurements (I_{v_m}). We used second-order spherical harmonics for the nominal model, which are a function of the local time and geomagnetic latitude of the IPP. The model is formulated as Equation (3) (Hobson, 1931).

$$\hat{I}_0(\Phi_m, t_{local}) = \sum_{n=0}^{2} \left\{ \sum_{m=0}^{n} \{C_{nm}\cos(m \cdot t_{local}) + S_{nm}\sin(m \cdot t_{local})\} P_{nm}(\sin(\Phi_m)) \right\}. \tag{3}$$

We can simplify Equation (3) by using the following definitions.

$$h_1 \equiv \sin(\Phi_m), \quad h_2 \equiv \cos(\Phi_m), \quad h_3 \equiv \sin(t_{local}), \quad h_4 \equiv \cos(t_{local}). \tag{4}$$

Now, Equation (3) can be rearranged into simple fourth-order polynomials as Equation (5).

$$\begin{aligned}\hat{I}_0(\Phi_m, t_{local}) = {} & C_{00} + C_{10} \cdot h_1 + (C_{11} \cdot h_4 + S_{11} \cdot h_1) \cdot h_2 + \frac{C_{20}}{2}(3h_1^2 - 1) \\ & + (C_{21}h_4 + S_{21}h_3) \cdot (3h_1h_2) + 3h_2^2(C_{22}(2h_4^2 - 1) + S_{22}(2h_3h_4)).\end{aligned} \tag{5}$$

https://doi.org/10.1017/S0373463302001741 Published online by Cambridge University Press

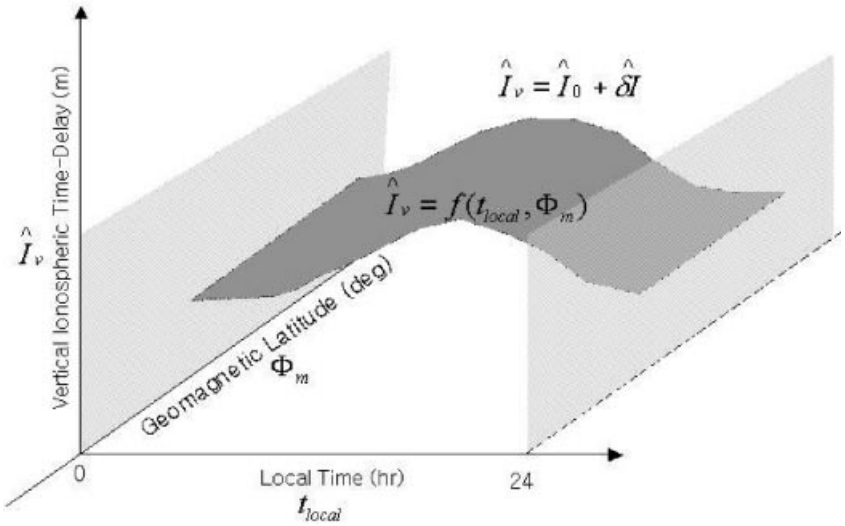


Figure 3. Coordinates of ionospheric time-delay model.

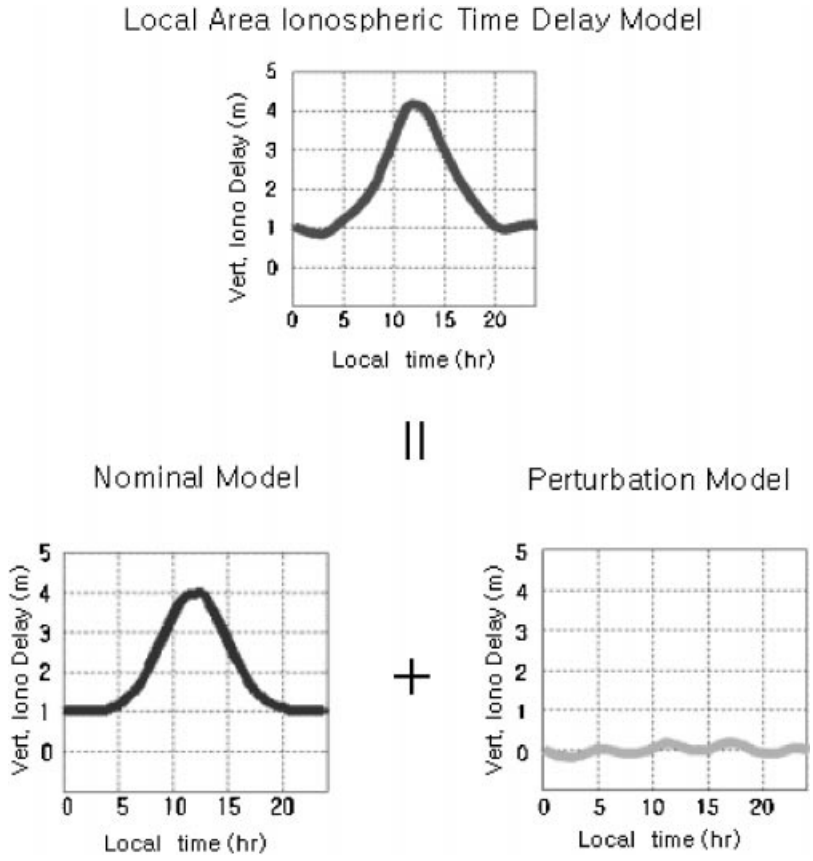


Figure 4. Concept of local-area ionospheric time-delay model (sum of nominal and perturbation model).

https://doi.org/10.1017/S0373463302001741 Published online by Cambridge University Press

Second-order spherical harmonics are therefore not too complex to be used by the reference station or the users. In addition, Equation (5) has some merits. The first is filter stability. If we use Equation (5) as the nominal ionospheric time-delay model, we can use a linear recursive least-square filter for parameter estimation. This filter is asymptotically stable regardless of initial conditions (Brown and Hwang, 1985). The second is continuity with respect to the local time axis. The non-linear functions that were used as nominal ionospheric time-delay model candidates in our previous paper (Kee and Yun, 1997) were not continuous at time zero. This was because they had no periodic characteristics on the local time axis. However, there is no discontinuity problem for spherical harmonics, because they use trigonometric functions and local time is normalized between 0 and 2π (mapping 0-hour to 0 and 24-hour to 2π).

To estimate L1/L2 inter-frequency biases and nominal model parameters using a weighted recursive least-square estimator (Astrom and Wittenmark, 1995), we define an observation matrix ($\underline{H}_k$) as Equation (6), estimate state vector ($\underline{x}_k$) as Equation (7), and the measurement vector ($\underline{z}_k$) as Equation (8).

$$\underline{H}_k = \begin{bmatrix} F(\theta_k^{SV_1}) \cdot \underline{I_v}_k^{SV_1} & 1 & -1 & 0 & 0 & \cdots & 0 \\ F(\theta_k^{SV_2}) \cdot \underline{I_v}_k^{SV_2} & 1 & 0 & -1 & 0 & \cdots & 0 \\ \vdots & \vdots & \vdots & \vdots & \vdots & \ddots & \vdots \\ F(\theta_k^{SV_n}) \cdot \underline{I_v}_k^{SV_{32}} & 1 & 0 & 0 & 0 & \cdots & -1 \end{bmatrix}_{32\times 42} \tag{6}$$

where:

$$\underline{I_v}_k^{SV_i} = [1 \; h_{1k} \; h_{2k}h_{4k} \; h_{1k}h_{2k} \; (3h_{1k}^2-1)/2 \; 3h_{1k}h_{2k}h_{4k} \; 3h_{1k}h_{2k}h_{3k} \; 3h_{2k}^2(2h_{4k}^2-1) \; 6h_{2k}^2 \; h_{3k}h_{4k}]_{1\times 9}$$

$$h_{1k} = \sin(\Phi_m^{SV_{i_k}}), \quad h_{2k} = \cos(\Phi_m^{SV_{i_k}}), \quad h_{3k} = \sin(t_{local}^{SV_{i_k}}), \quad h_{4k} = \cos(t_{local}^{SV_{i_k}})$$

$$\underline{\hat{x}}_k^T = \left[C_{00k} \; C_{10k} \; C_{11k} \; S_{11k} \; C_{20k} \; C_{21k} \; S_{21k} \; C_{22k} \; S_{22k} \; \hat{I}_{b_{RXk}} \; \hat{I}_{b_{TXk}}^{SV_1} \cdots \hat{I}_{b_{TXk}}^{SV_{32}} \right]_{9\times 1} \tag{7}$$

$$\underline{z}_k^T = \left[I_{sm}^{SV_1k} \; I_{sm}^{SV_2k} \cdots I_{sm}^{SV_{32}k} \right]_{32\times 1}. \tag{8}$$

If there is no measurement for the ith satellite, both $I_{sm}^{SV_1k}$ of $\underline{z}_k$ and $F(\theta_k^{SV_i})$ of $\underline{H}_k$ should be set to zero. With this trick, it is not necessary to change the sizes of $\underline{\hat{x}}_k$, $\underline{z}_k$ and $\underline{H}_k$ according to the number of visible satellites. As there are 32 PRN numbers, $\underline{H}_k$ has 32 rows and 42 columns. The number of columns comprises the sum of the nine nominal model parameters and 33 L1/L2 inter-frequency biases of the GPS receiver and all the satellites. Therefore, the first nine elements of $\underline{\hat{x}}_k$ are nominal model parameters and the remaining 33 are L1/L2 inter-frequency biases of the GPS receiver and each satellite.

At the kth epoch, the weighted recursive least-square estimation filter is described as Equation (9).

$$\begin{aligned} \underline{\hat{x}}_{k+1} &= \underline{\hat{x}}_k + \underline{R}_{k+1}^{-1} \cdot \underline{H}_{k+1}^T \cdot \underline{W}_{k+1}^{-1} \cdot \left[\underline{z}_{k+1} - \underline{H}_{k+1} \cdot \underline{\hat{x}}_k \right] \\ \underline{R}_{k+1} &= \underline{R}_k + \underline{H}_{k+1}^T \cdot \underline{W}_{k+1}^{-1} \cdot \underline{H}_{k+1}. \end{aligned} \tag{9}$$

https://doi.org/10.1017/S0373463302001741 Published online by Cambridge University Press

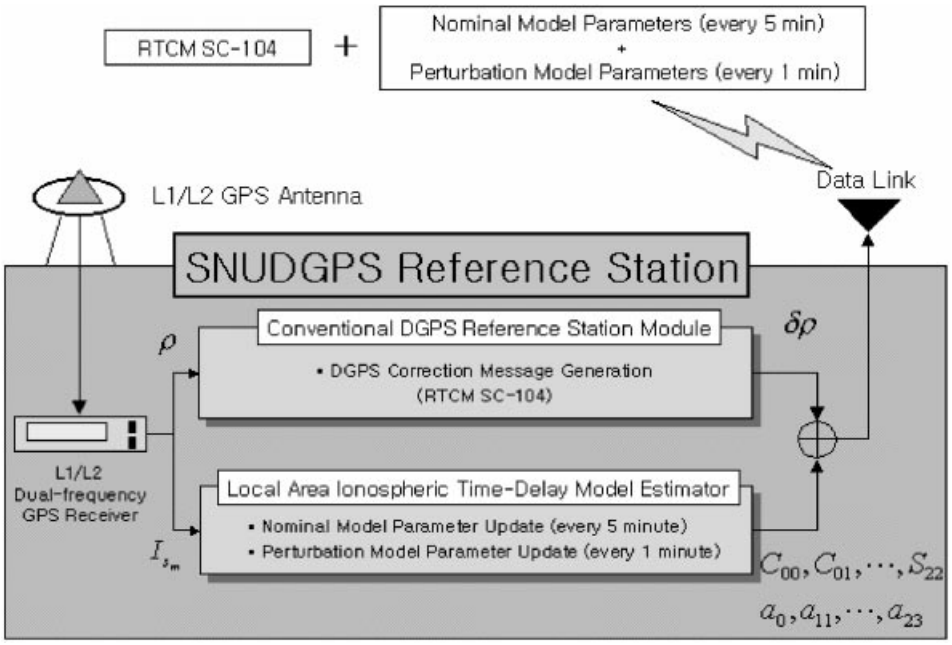


Figure 5. SNUDGPS reference station.

In Equation (9), $\underline{W}_k$ is a measurement covariance matrix. For the Trimble 4000 series receiver, it can be expressed as a function of satellite elevation angle (Kee *et al*., 1996).

$$\underline{W}_k = \begin{bmatrix} \sigma^{SV_{1_k}{}^2} & 0 & \cdots & 0 \\ 0 & \sigma^{SV_{2_k}{}^2} & \cdots & 0 \\ \vdots & \vdots & \ddots & \vdots \\ 0 & 0 & 0 & \sigma^{SV_{32_k}{}^2} \end{bmatrix} \tag{10}$$

where: $\sigma^{SV_{i_k}{}^2} = x_0 + x_1 \cdot e^{\left(-\frac{\theta^{SV_{i_k}}}{x_2}\right)}$, $x_0 = 0{\cdot}24$, $x_1 = 3{\cdot}88$, $x_2 = 9{\cdot}65$.

As Equation (9) is asymptotically stable, the filter converges as the number of measurements increases. The initial value of $\underline{\hat{x}}_0$, $\underline{R}_0$ can be assigned arbitrarily provided that $\underline{R}_0$ is positive definite, and it takes 1–2 days for this filter to settle. For convenience, the zero-vector is used for $\underline{\hat{x}}_0$ and the identity matrix is used for $\underline{R}_0$. It should be noted that this filter must be reset periodically. Because Equation (9) is just a sequential version of least-square fitting, $\underline{R}_k$ should be reset as $\underline{R}_0$ periodically to follow the changes of ionosphere activity and L1/L2 inter-frequency biases (Astrom and Wittenmark, 1995). The appropriate reset period is about one week. We should reset only $\underline{R}_k$ and conserve $\underline{\hat{x}}_k$ to use local-area ionospheric time-delay model parameters continuously.

2.2.3. *Perturbation ionospheric time-delay model and parameter estimation filter*. As the nominal model is a least-square fit over several days, it is not able to describe rapid changes of the ionospheric time delay. A supplementary part is therefore necessary to describe short-period changes of ionospheric time delay. To achieve this, we designed a perturbation ionospheric time-delay model with a time constant of

https://doi.org/10.1017/S0373463302001741 Published online by Cambridge University Press

three hours. A perturbation is the difference between the measured vertical ionospheric time delay and the nominal model-based ionospheric time delay. We can measure the perturbation by subtracting the nominal model-based ionospheric time delay from the measured vertical ionospheric time delay as shown in Equation (11).

$$\delta I_m(\Phi_m, t_{local}) = I_{v_m}(\Phi_m, t_{local}) - \hat{I}_0(\Phi_m, t_{local}). \tag{11}$$

We have used second-order geomagnetic latitude (Φ_m) and local time (t_{local}) polynomials in the perturbation model. Equation (12) is the perturbation model and there are six parameters.

$$\delta\hat{I}(\Phi_m, t) = a_0 + a_{11} \cdot t_{local} + a_{12} \cdot \Phi_m + a_{21} \cdot t_{local}^2 + a_{22} \cdot \Phi_m^2 + a_{23} \cdot t_{local} \cdot \Phi_m. \tag{12}$$

To estimate those parameters, we have used a recursive least-square filter with exponential forgetting. The forgetting characteristics make it unnecessary to reset the filter periodically as in the nominal model parameter estimation filter.

We define the observation matrix $\underline{\phi}_k$ as Equation (13), estimate state vector $\underline{\hat{\theta}}_k$ as Equation (14), and the measurement vector $\underline{z}_k$ as Equation (15) for m visible satellites.

$$\underline{\phi}_k = \begin{bmatrix} 1 & t_{local}^{SV_{1k}} & \Phi_m^{SV_{1k}} & t_{local}^{2\,SV_{1k}} & \Phi_m^{2\,SV_{1k}} & t_{local}^{SV_{1k}} \cdot \Phi_m^{SV_{1k}} \\ 1 & t_{local}^{SV_{2k}} & \Phi_m^{SV_{2k}} & t_{local}^{2\,SV_{2k}} & \Phi_m^{2\,SV_{2k}} & t_{local}^{SV_{2k}} \cdot \Phi_m^{SV_{2k}} \\ \vdots & \vdots & \vdots & \vdots & \vdots & \vdots \\ 1 & t_{local}^{SV_{mk}} & \Phi_m^{SV_{mk}} & t_{local}^{2\,SV_{mk}} & \Phi_m^{2\,SV_{mk}} & t_{local}^{SV_{mk}} \cdot \Phi_m^{SV_{mk}} \end{bmatrix}_{m\times 6} \tag{13}$$

$$\underline{\hat{\theta}}_k^T = [a_{0k}\ a_{11k}\ a_{12k}\ a_{21k}\ a_{22k}\ a_{23k}]_{6\times 1} \tag{14}$$

$$\underline{z}_k^T = [\delta I_m^{SV_{1k}}\ \delta I_m^{SV_{2k}} \cdots \delta I_m^{SV_{mk}}]_{m\times 1}. \tag{15}$$

At the kth epoch, the propagation equation of the recursive least-square filter with exponential forgetting is Equation (16) (Astrom and Wittenmark, 1995).

$$\begin{aligned} \underline{\hat{\theta}}_{k+1} &= \underline{\hat{\theta}}_k + \underline{R}_k^{-1} \cdot \underline{\phi}_{k+1}^T \cdot \left[\underline{z}_{k+1} - \underline{\phi}_{k+1} \cdot \underline{\hat{\theta}}_k\right] \\ \underline{R}_{k+1} &= \lambda \cdot \underline{R}_k + \underline{\phi}_{k+1}^T \cdot \underline{\phi}_{k+1}. \end{aligned} \tag{16}$$

In the above equation, the exponential forgetting parameter (λ) is defined as Equation (17) (Astrom and Wittenmark, 1995).

$$\lambda = e^{-\frac{\Delta t}{T_f}}. \tag{17}$$

If the sampling period (Δt) of raw data is one second and the time-constant (T_f) of the exponential forgetting parameter is three hours, the exponential forgetting parameter (λ) is about 9·999. We used three hours as the filter time-constant. Because Equation (16) is also asymptotically stable, the filter converges as the number of measurements increases, so the initial value of $\underline{\hat{\theta}}_0$, $\underline{R}_0$ can be assigned arbitrarily provided that $\underline{R}_0$ is positive definite. For convenience, the zero-vector is used for $\underline{\hat{\theta}}_0$ and the identity matrix is used for $\underline{R}_0$.

2.3. *The tropospheric time-delay model.* We used Black's tropospheric time-delay model (Black, 1978). This model is a function of satellite elevation angle (θ),

https://doi.org/10.1017/S0373463302001741 Published online by Cambridge University Press

altitude (h_a), temperature (T_c), and pressure (P_a). We used standard atmospheric conditions for the tropospheric time-delay correction. Black's model is the sum of wet (d_{s_w}) and dry (d_{s_d}) components as shown in Equation (18).

$$\hat{t} = d_{s_w}(\theta, h_a, T_c, P_a) + d_{s_d}(\theta, h_a, T_c, P_a) \tag{18}$$

where:

$$d_{s_w} = \frac{1}{\sqrt{1 - \left\{ \cos\theta \Big/ \left(1 + \frac{13 \times 10^3 (1 - l_c)}{r_e + h_a} \right) \right\}^2}} \cdot k_w \cdot \left(1 - \frac{h_a}{13 \times 10^3} \right)^5$$

$$d_{s_d} = \frac{2{\cdot}343 \times P_a}{\sqrt{1 - \left\{ \cos\theta \Big/ \left(1 + \frac{148{\cdot}98 \times (T_k - 4{\cdot}12) \times (1 - l_c)}{r_e + h_a} \right) \right\}^2}} \cdot \frac{T_k - 4{\cdot}12}{T_k} \cdot \left(1 - \frac{h_a}{148{\cdot}98 \times (T_k - 4{\cdot}12)} \right)^5$$

$$l_c = 0{\cdot}83$$

$$k_w = \begin{cases} 0{\cdot}28: \text{summer in tropics or mid-latitudes} \\ 0{\cdot}20: \text{spring or fall in mid-latitudes} \\ 0{\cdot}12: \text{winter in maritime mid-latitudes} \\ 0{\cdot}06: \text{winter in continental mid-latitudes} \\ 0{\cdot}05: \text{polar regions.} \end{cases}$$

This model is an algebraic function and all the parameters are known. It may seem that an iterative method is required to calculate the user's position, because the altitude (h_a) appears in Equation (18). However, an approximate DGPS solution is sufficient for tropospheric time delay correction so it is not necessary to use an iterative method.

3. SNUDGPS (SEOUL NATIONAL UNIVERSITY DIFFERENTIAL GPS).

Using the local-area ionospheric time-delay model ($\hat{I}_v$) and the tropospheric time-delay model ($\hat{t}$), we have modified DGPS pseudo-range corrections ($\delta\rho_{DGPS}$). In other words, pseudo-range corrections are made more accurate by use of atmospheric time-delay models. This is the key idea of SNUDGPS.

In SNUDGPS, the reference station calculates not only DGPS pseudo-range corrections ($\delta\rho_{DGPS}$), but also local-area ionospheric time-delay model parameters ($C_{00}, C_{01}, \ldots, S_{22}, a_0, a_{11}, \ldots, a_{23}$). All this information is transmitted to SNUDGPS users so they can make SNUDGPS pseudo-range corrections ($\delta\rho_{SNUDGPS}$), using DGPS pseudo-range corrections ($\delta\rho_{DGPS}$), the local-area ionospheric time-delay model ($\hat{I}_v$), and the tropospheric time-delay model ($\hat{t}$). More details are given in the following sections.

3.1. *SNUDGPS Reference Station.*

Figure 5 (See Page 311) shows the structure of the SNUDGPS reference station, which has two modules. One calculates the pseudo-range corrections ($\delta\rho_{DGPS}$) and transmits them using the RTCM SC-104 protocol. It is a conventional DGPS reference station module. The other module estimates the local-area ionospheric time-delay model parameters ($C_{00}, C_{01}, \ldots, S_{22}, a_0, a_{11}, \ldots, a_{23}$). All the parameters can be transmitted to users by adding only two

https://doi.org/10.1017/S0373463302001741 Published online by Cambridge University Press

messages to the RTCM SC-104 protocol. The first message transmits the nine nominal model parameters (C_{00}, C_{01}, … , S_{22}) every five minutes. The second message transmits the six perturbation model parameters (a_0, a_{11}, … , a_{23}) every minute.

To implement the local-area ionospheric time-delay model estimator in Figure 5, the SNUDGPS reference station should have a L1/L2 dual-frequency GPS receiver that can measure ionospheric time delays. Thus, any DGPS reference station that has a L1/L2 dual-frequency GPS receiver can be changed into a SNUDGPS reference station without installation of additional hardware. Only the software requires modification by implementing the real-time parameter estimation filter, and adding two messages to the RTCM SC-104 protocol. Figure 6 shows the structure of the

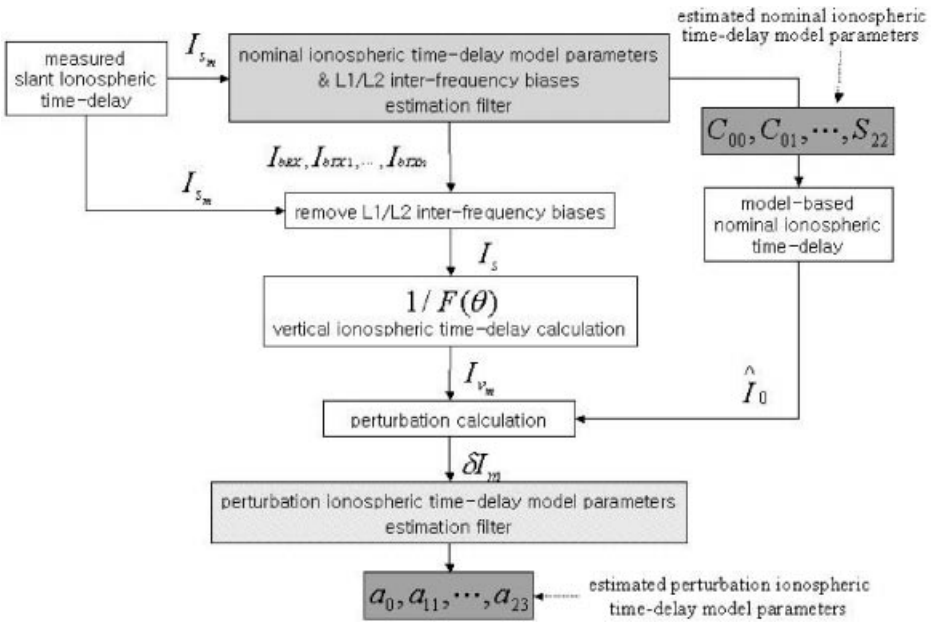


Figure 6. Local-area ionospheric time-delay model parameter estimation filter.

local-area ionospheric time-delay model parameter estimation filter with its two sub-filters. The first is a recursive least-square estimator that estimates L1/L2 inter-frequency biases ($I_{b_{RX}}$, $I_{b_{RX_1}}$, … , $I_{b_{RX_n}}$) and nominal ionospheric time-delay model parameters (C_{00}, C_{01}, … , S'_{22}). Equation (9) is the propagation equation. From the states of Equation (9), we can calculate vertical ionospheric time delays (I_{v_m}), model-based nominal ionospheric time delays ($\hat{I}_0$), and perturbations (δI_m) of all visible satellites. Using these perturbation measurements, the second sub-filter estimates the perturbation ionospheric time-delay model parameters (a_0, a_{11}, … , a_{23}). This sub-filter is a recursive least-square estimator with exponential forgetting, and Equation (16) is the propagation equation.

As mentioned in 2.2.2., it takes 1–2 days for the SNUDGPS reference station filter to settle from a cold start. This settling time is required by the first sub-filter. The SNUDGPS reference station must therefore operate in DGPS mode until the first sub-filter settles. However, a warm start does not take as long because L1/L2 inter-

https://doi.org/10.1017/S0373463302001741 Published online by Cambridge University Press

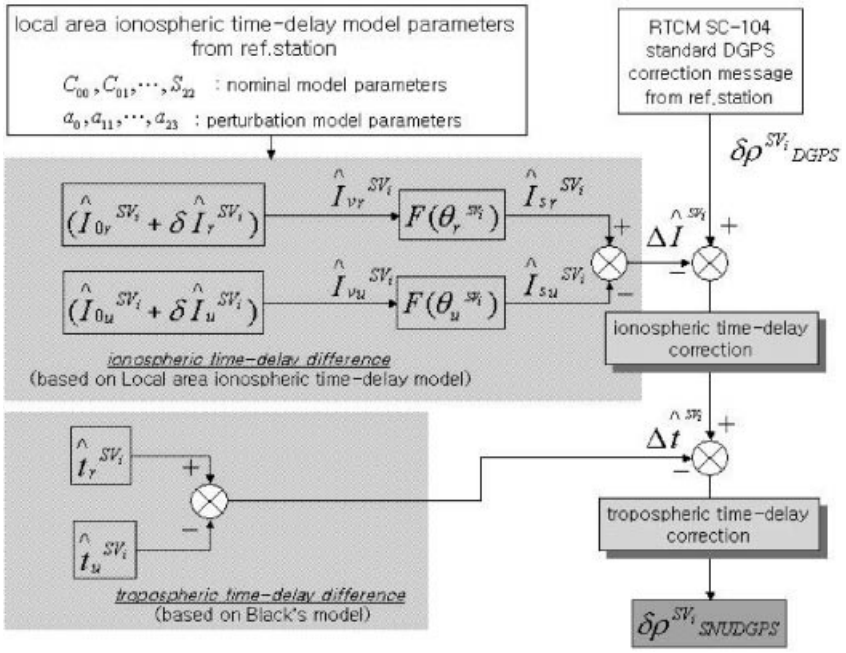


Figure 7. SNUDGPS pseudo-range correction for *i*th satellite.

frequency biases and the ionospheric time delay do not change over short time periods.

3.2. *SNUDGPS User*. DGPS and SNUDGPS positioning algorithms are the same except that DGPS uses $\delta\rho_{DGPS}$ and SNUDGPS uses $\delta\rho_{SNUDGPS}$ as pseudo-range corrections. It is therefore only necessary to explain how to calculate $\delta\rho_{SNUDGPS}$ in this paper.

SNUDGPS pseudo-range corrections ($\delta\rho_{SNUDGPS}$) can be calculated by using three components: DGPS pseudo-range corrections ($\delta\rho_{DGPS}$), the local-area ionospheric time-delay model, and the tropospheric time-delay model. Figure 7 and Equation (19) show the relationship between $\delta\rho_{SNUDGPS}$ and $\delta\rho_{DGPS}$ for one visible satellite.

$$\delta\rho_{SNUDGPS} = \delta\rho_{DGPS} - \Delta\hat{I} - \Delta\hat{t} \tag{19}$$

where:

$$\Delta\hat{I} = \hat{I}_r - \hat{I}_u = F(\theta_r) \cdot (\hat{I}_{0_r} + \delta\hat{I}_r) - F(\theta_u) \cdot (\hat{I}_{0_u} + \delta\hat{I}_u)$$
$$\Delta\hat{t} = \hat{t}_r - \hat{t}_u.$$

In Figure 7 and Equation (19), $\Delta\hat{I}$ is the ionospheric time-delay difference between the reference station and the user. This difference can be calculated from the local-area ionospheric time-delay model, which is the sum of the nominal and perturbation models. All the parameters are transmitted from the reference station periodically. As the ionospheric time delay is included in the pseudo-range, we must use the slant ionospheric time delay, which is the product of the vertical ionospheric time delay and an obliquity factor, to calculate $\Delta\hat{I}$ as shown in Figure 7 and Equation (19). The value of $\Delta\hat{t}$ is the tropospheric time-delay difference between the reference station and the user. We can calculate these differences algebraically using the tropospheric time-

https://doi.org/10.1017/S0373463302001741 Published online by Cambridge University Press

delay model for all visible satellites. By subtracting $\Delta\hat{I}$ and $\Delta\hat{t}$ from $\delta\rho_{DGPS}$, $\delta\rho_{SNUDGPS}$ is then obtained. This algorithm can easily be implemented in a GPS receiver by adding a few lines of source code to the DGPS correction module.

3.3. *Experimental results.* We analyzed the performance of the local-area ionospheric time-delay model and SNUDGPS accuracy using experimental data. Table 1 is a summary of the experimental data. To measure the ionospheric time

Table 1. Experimental data.

	Reference station	User
Location	SNU, Seoul	Hallym, Cheju
Latitude[a]	37° 26′ 58·911″ N	35° 24′ 25·832″ N
Longitude[a]	126° 57′ 09·80″ E	126° 15′ 17·12″ E
Height[a]	282·620 m	32·946 m
Date	January 28, 1998 – February 2, 1998	
Receiver	Trimble 4000ssi (L1/L2 Dual-frequency)	
Sampling Time	1 sec	

[a]WGS-84 based latitude, longitude, and height.

delay, we used L1/L2 dual-frequency GPS receivers. The L2 data of the user's receiver were used only for error analysis. As the Trimble 4000ssi GPS receiver measures dual-frequency data using the codeless method, multi-path error becomes large when the satellite elevation angle is low. The elevation mask angle must therefore be chosen so that the ionospheric time delay can be measured accurately (Wilson and Mannucci, 1994). By trial and error, we determined the mask angle of the SNUDGPS reference station as 30 degrees. In other words, L1/L2 inter-frequency biases and local-area ionospheric time-delay model parameters have been estimated with data from satellites whose elevation angles were larger than 30 degrees.

To analyze SNUDGPS accuracy, we collected data at the reference and user stations simultaneously. The user's true position was calculated by use of a commercial survey program. Its accuracy is better than a few centimetres, so that its result can be considered as a true value for error analysis. Table 2 summarizes the

Table 2. Baseline survey result.[b]

	DN	dE	dU	Length
Baseline Components (metres)	−447902·01	−64924·74	−16377·83	452879·31
Standard Deviations	0·001760	0·002189	0·001927	0·001279

[b]Survey program is Trimble's ©GPSurvey and solution method is 'iono-free fixed double difference'.

baseline survey result. According to Table 2, the baseline length is about 453 km. This is much longer than the DGPS baseline limit of 100 km. We can expect serious positioning errors if we use DGPS.

3.4. *Local-area ionospheric time-delay model.* We applied the local-area ionospheric time-delay model parameter estimation filter to the experimental data. As it takes 1–2 days for this filter to settle, we plotted results starting 45 hours from the

https://doi.org/10.1017/S0373463302001741 Published online by Cambridge University Press

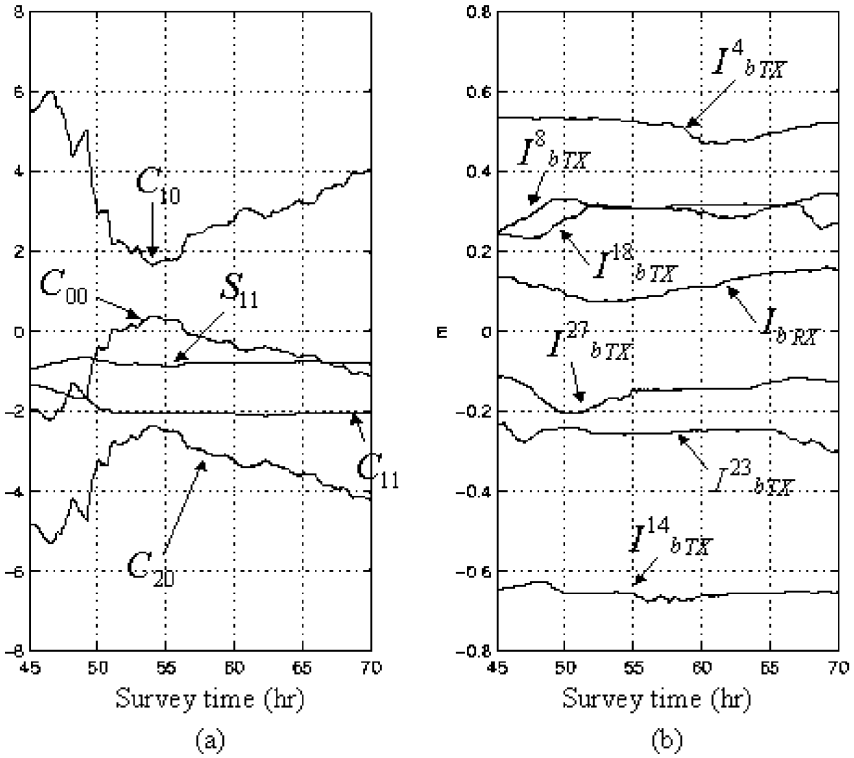


Figure 8. Estimated state: (a) Nominal ionospheric time-delay model parameters; (b) L1/L2 inter-frequency biases.

time the filter was turned on. Figure 8 is a time-history of the estimated state from the first sub-filter Equation (9). Figure 8(a) shows the first five nominal ionospheric time-delay model parameters, and (b) shows the L1/L2 inter-frequency biases of the GPS receiver and some satellites. As mentioned in the *Theory* section, L1/L2 inter-frequency biases are nearly constant. To check this result, we compared these estimated L1/L2 inter-frequency biases with those of Deutschen Zentrum für Luft und Raumfahrt (DLR) (http://www.nz.dlr.de/gps/gps-ion.html) and found that they match very well.

Figure 9(a) shows the nominal ionospheric time-delay model estimated at final time. It has its peak value at about 14 hours in the local time axis. This is consistent with Klobuchar's model. Figure 9(b) shows the perturbation ionospheric time-delay model estimated at final time. It shows higher values at lower geomagnetic latitudes and lower values at higher geomagnetic latitudes. This is because the ionospheric time delay of low latitude regions is larger than that of high latitude regions.

To evaluate model performance quantitatively, we calculated mean and RMS values of residuals. Figure 10(a) shows measured vertical ionospheric time delays (I_{v_m}), which are free from L1/L2 inter-frequency biases. Figure 10(b) shows model-based vertical ionospheric time delays ($\hat{I}_v$), which are sums of nominal and perturbation ionospheric time-delay model values. We defined the vertical residuals as the differences between these two values and plotted them in Figure 10(c). Figure

https://doi.org/10.1017/S0373463302001741 Published online by Cambridge University Press

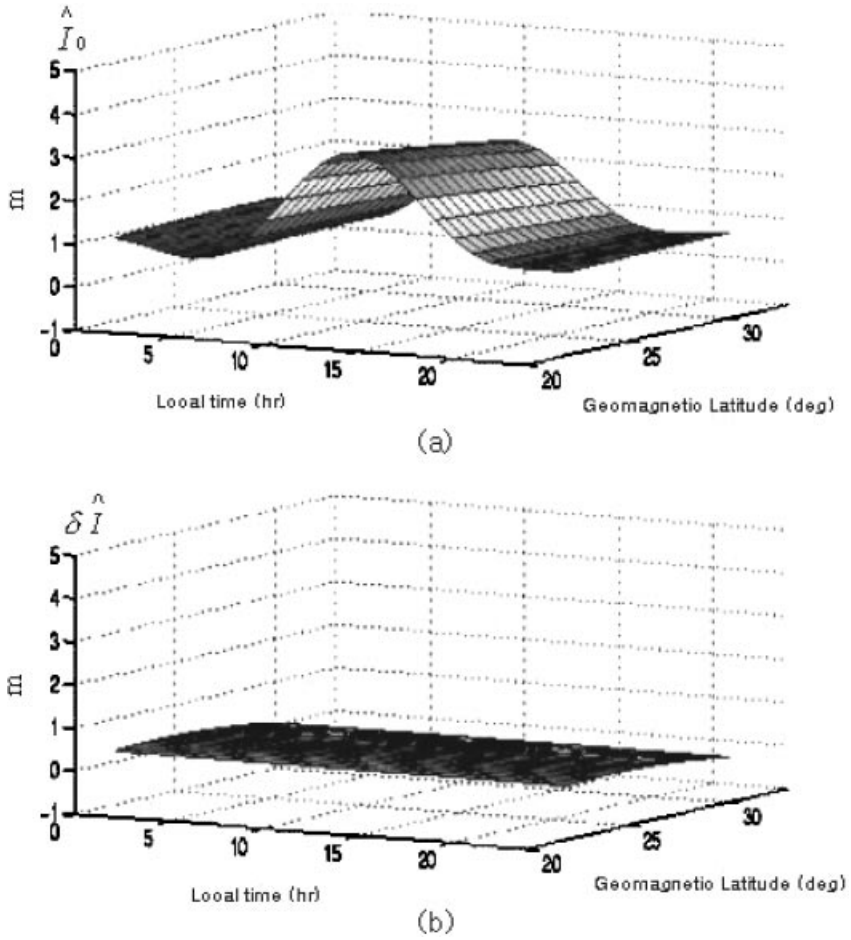


Figure 9. (a) Nominal ionospheric time-delay model at final time;
(b) Perturbation ionospheric time-delay model at final time.

10(d) shows slant residuals, which we defined as the product of vertical residuals and obliquity factors. We calculated mean and RMS values of these residuals and summarized them in Table 3, which shows that the local-area ionospheric time-delay model describes ionospheric time delays so well that we can use this model in SNUDGPS.

3.5. *Positioning performance comparison*: *SNUDGPS vs. DGPS.* We calculated the user's position using both DGPS and SNUDGPS at every epoch. In this processing, the SNUDGPS reference station updated the local-area ionospheric time-delay model parameters every epoch, but the user updated nominal model parameters every five minutes and updated the perturbation model parameters every minute. We also assumed that there were no time delays for data transmission from the reference station to the user. We used the baseline survey result of Table 2 as the user's true position for the error analysis.

Figure 11 shows DGPS positioning errors and Figure 12 shows SNUDGPS positioning errors. As atmospheric time delay is a kind of slowly changing bias,

https://doi.org/10.1017/S0373463302001741 Published online by Cambridge University Press

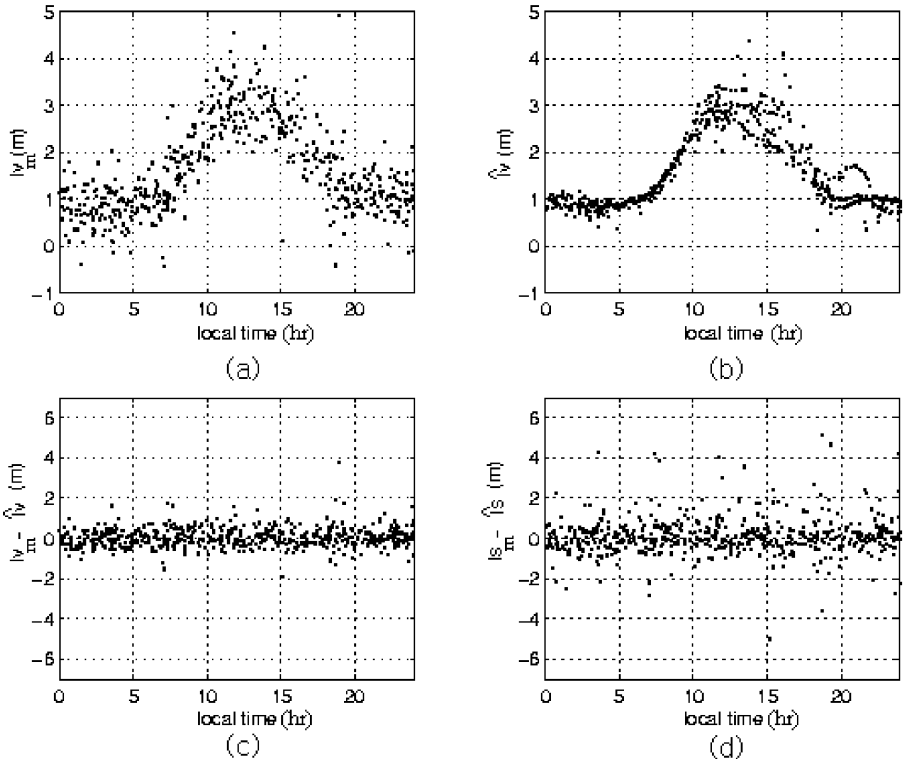


Figure 10. Local area ionospheric time-delay model performance: (a) Measured vertical ionospheric time-delay; (b) Model-based vertical ionospheric time-delay; (c) Vertical residual; (d) Slant residual.

Table 3. Local-area ionospheric time-delay model performance.

	Vertical residual	Slant residual
Mean	0·0265 m	0·0667 m
RMS	0·4962 m	1·0277 m

DGPS positioning errors tend to be biased for a user far from the reference station. In Figure 11, DGPS positioning errors are biased. If we consider that the baseline-length between the SNU reference station and the user is more than 400 km, we can expect this result. However, there are no biases in Figure 12. This means that atmospheric errors were successfully removed by using SNUDGPS.

We have summarized the error analysis result in Table 4. According to Table 4, the mean and RMS values of SNUDGPS positioning errors were reduced to at least half the DGPS positioning errors. With this result, we can conclude that SNUDGPS can extend coverage of DGPS to more than 100 km and is a more accurate system than DGPS.

4. CONCLUSIONS. To compensate the ionospheric spatial de-correlation problem of conventional DGPS, we have developed a local-area ionospheric time-

https://doi.org/10.1017/S0373463302001741 Published online by Cambridge University Press

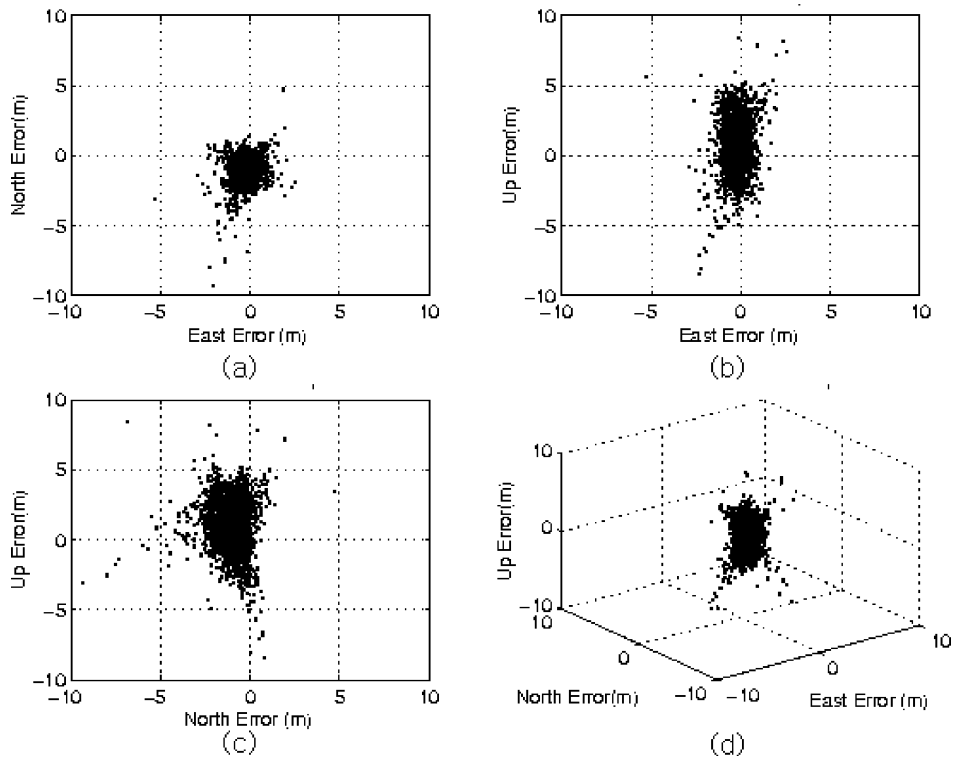


Figure 11. DGPS positioning error: (a) North-East plane error; (b) East-up plane error; (c) North-up plane error; (d) 3-D error.

Table 4. Positioning error analysis (DGPS vs SNUDGPS).

	Mean			RMS		
	North	East	Up	North	East	Up
DGPS	−0·9861 m	−0·2496 m	0·8308 m	1·2566 m	0·5135 m	1·7529 m
SNUDGPS	0·3907 m	−0·0320 m	0·0444 m	0·6206 m	0·3211 m	0·9210 m

delay model. This model consists of nominal and perturbation time-delay models. All the parameters were estimated at the SNUDGPS reference station by use of on-line filters. Experimental results showed that the local-area ionospheric time-delay model describes real ionospheric time delays with an accuracy of 1·03 m (RMS). With this model and Black's tropospheric time-delay model, we have modified the DGPS correction algorithm. The new algorithm's name is SNUDGPS. SNUDGPS users can compensate atmospheric time-delay differences between a reference station and themselves by use of these models. Experimental error analysis showed that the mean of positioning error was reduced from 1·36 m (DGPS) to 0·39 m (SNUDGPS) and the RMS value was reduced from 2·21 m (DGPS) to 1·15 m (SNUDGPS). In this experiment, the baseline-length was about 453 km, which is much longer than the DGPS baseline-limit of 100 km. This proves that coverage of DGPS can be extended

https://doi.org/10.1017/S0373463302001741 Published online by Cambridge University Press

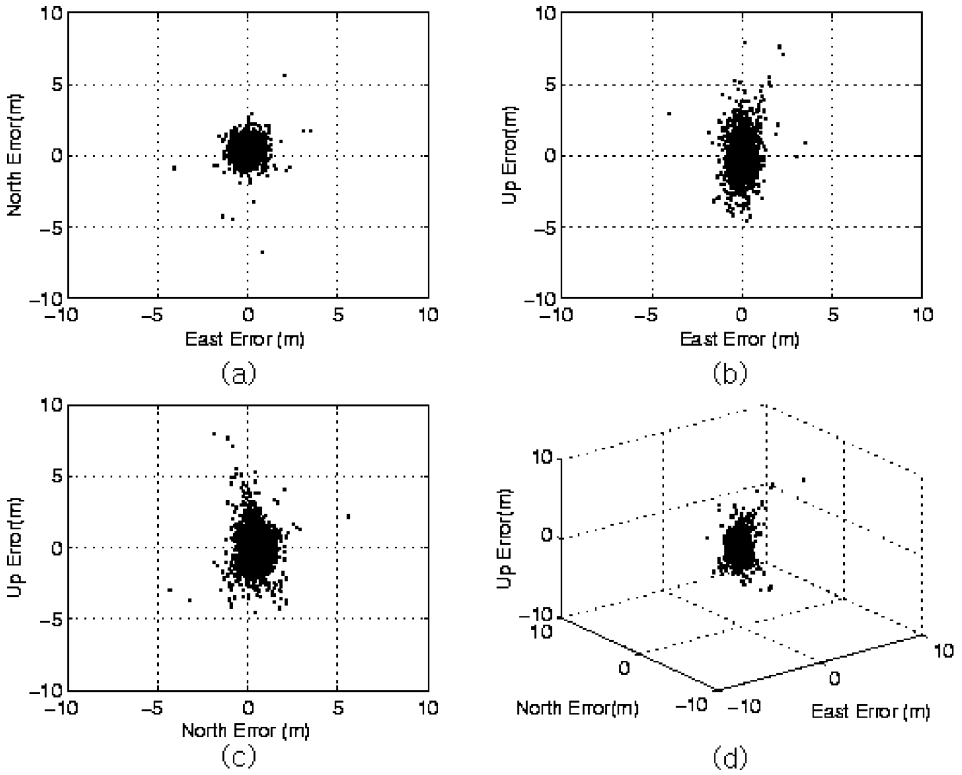


Figure 12. SNUDGPS positioning error: (a) North-East plane error; (b) East-up plane error; (c) North-up plane error; (d) 3-D error.

to more than 100 km by use of SNUDGPS. This allows SNUDGPS to be implemented with a smaller number of reference stations than DGPS for the same area. Furthermore, SNUDGPS can be implemented easily by adding only a simple firmware modification to the user's GPS receiver and two additional messages to the RTCM SC-104 DGPS protocol. Therefore, SNUDGPS is a more accurate and more economical choice, because coverage can be extended to more than twice that of DGPS by the use of atmospheric time-delay models. We recommend that SNUDGPS be used as an intermediary system between Local Area Augmentation System (LAAS) and Wide Area Augmentation System (WAAS).

ACKNOWLEDGEMENT

This research was supported by a grant from the BK-21 Program for Mechanical and Aerospace Engineering Research at Seoul National University.

REFERENCES

ARINC Research Corporation (1993). *NAVSTAR GPS space segment/navigation user interfaces*. Drawing No. ICD-GPS-200, REV. C, pp. 126–127.

Astrom, K. and Wittenmark, B. (1995). *Adaptive control*, 2nd edition, Addison Wesley Publishing Company, pp. 42–56.

Black, H. D. (1978). An easily implemented algorithm for the tropospheric range correction. *Journal of Geophysical Research*, Vol. 83, No. B4, pp. 1825–1828.

https://doi.org/10.1017/S0373463302001741 Published online by Cambridge University Press

Brown, R. and Hwang, P. (1985). *Introduction to Random Signals and Applied Kalman Filtering*, John Wiley & Sons, pp. 242–288.

Chao, Y., Tsai, Y., Walter, T., Kee, C., Enge, P. and Parkinson, B. (1995). The ionospheric model improvement of the Stanford WAAS network. *Proceedings of National Technical Meeting*, Institute of Navigation, Anaheim, pp. 531–538.

Coco, D., Coker, C., Dahlke S. and Clynch, J. (1991). Variability of GPS satellites differential group delay biases. *IEEE Transactions on Aerospace and Electronic systems*, Vol. 27, No. 6, pp. 931–938.

Hobson, E. (1931). *The Theory of Spherical and Elliptical Harmonics*, Cambridge University Press, pp. 777–778.

Kee, C. (1995). Wide Area Differential GPS. *Global Positioning System Theory and Applications Volume II*, edited by Parkinson, B. W. and Spilker, J. J., Jr., Vol. 164, Progress in Astronautics and Aeronautics, AIAA, pp. 81–115.

Kee, C., Walter, T., Enge, P. and Parkinson, P. (1996). Quality control algorithms on wide-area reference station for WAAS. *Proceedings of 52nd ION Annual Meeting*, Cambridge, Massachusetts, pp. 487–495.

Kee, C. and Yun, D. (1997). Development of local ionospheric time delay model for single-frequency DGPS users. *Proceedings of ION GPS-97*, Kansas City, Missouri, pp. 1113–1122.

Klobuchar, J. A. (1987). Ionospheric time-delay algorithms for single-frequency GPS users. *IEEE Transactions on Aerospace and Electronic systems*, Vol. AES-23, No. 3, pp. 325–331.

Klobuchar, J. A. (1995). Ionospheric effects on GPS. *Global Positioning System Theory and Applications Volume I*, edited by Parkinson, B. W. and Spilker, J. J., Jr., Vol. 164, Progress in Astronautics and Aeronautics, AIAA, pp. 485–515.

Qiu, W., Lachapelle, G. and Cannon, M. E. (1994). Ionospheric effect modelling for single frequency GPS users. *Proceedings of National Technical Meeting*, Institute of Navigation, San Diego, pp. 911–919.

Wilson, B. and Mannucci, A. (1993). Instrumental biases in ionospheric measurements derived from GPS data. *Proceedings of ION GPS-93*, Salt Lake City, Utah, pp. 1343–1351.

Wilson, B. and Mannucci, A. (1994). Extracting ionospheric measurements from GPS in the presence of anti-spoofing. *Proceedings of ION GPS-94*, Salt Lake City, Utah, pp. 1599–1608.

https://doi.org/10.1017/S0373463302001741 Published online by Cambridge University Press